ROMANIAN JOURNAL OF INFORMATION SCIENCE AND TECHNOLOGY
Volume **24**, Number 2, 2021, 233–243

Fabrication of Fresnel lenses operating as image correcting optical components for long infrared imaging systems

R. REBIGAN[1], A. AVRAM[1], R. TUDOR[1], M. KUSKO[1], D. URSU[2], G. SOROHAN[2], and C. KUSKO[1]

[1]National Institute for R&D in Microtechnologies – IMT Bucharest, 126A Str. Erou Iancu Nicolae, Voluntari, Romania
[2]PRO OPTICA S. A., 67 Gh. Petrascu St., Bucharest, Romania
E-mail: cristian.kusko@imt.ro

Abstract. We present the technological processes required to fabricate silicon Fresnel lenses with sixteen discrete depth levels operating as corrector optical components for long infrared imaging systems. In order to configure the discrete surface of the lenses, four separated photolithographic processes each one of them followed by deep reactive ion etching were used. In order to detach the configured lenses presenting a disk like shape from the wafer, a DRIE Bosch deep etching process was employed. Finally, an antireflective layer consisting of a nanostructured surface was configured on both sides of the lenses in order to improve the transmission in LWIR spectral range. The geometrical parameters of the fabricated Fresnel lenses were determined by white light interferometry method and it was found that they are in good agreement with the design specifications. The optical and scanning electron microscopy measurements reveal a high quality of the optical surface with a low value of roughness. The spectral characteristics of the lenses in the LWIR spectral region reveal a transmission of above 70%.

Key-words: Fresnel lens, long infrared optics, silicon microfabrication, photolithographic processes, reactive ion etching.

1. Introduction

The radiation with the wavelength in the range of 8 -12 μm called long wavelength infrared (LWIR) presents a special interest for research and development since it allows imaging of objects whose temperatures are comparable with the room or environment temperatures without requiring additional illumination. Motivated by the applications of LWIR imaging in defense and

security, earth sciences, agriculture and environment monitoring, health, astronomy and space explorations, this area of optics emerged as one of the most active area in research and development, a strong drive for this field being the necessity of developing and manufacturing low cost, robust, reliable and sensitive LWIR imaging cameras [1].

The optical system of an LWIR imaging camera consists of lenses operating in infrared which are, generally, fabricated from expensive and hard to process materials such as germanium or dichalcogenide glasses, fact that contributes to an overall high cost of the infrared camera. Silicon presents a series of advantages such as low cost, ease of processing as well as the maturity of microfabrication technologies, being the material of choice for the mid infrared spectral range, namely 2 – 5 μm where it is transparent [2, 3]. Nevertheless, the presence of absorption bands in LWIR renders silicon unsuitable for the fabrication of bulk optical components in the LWIR spectral range, due to the fact that the considerable thickness of the infrared silicon lenses leads to an unacceptable attenuation of the optical field. A conceptual solution to the aforementioned challenge consists in dramatically reducing the thickness of the silicon optical components by configuring them on thin substrates such as double polished silicon wafers diminishing in this way the attenuation caused by the LWIR absorption bands.

For the thin optical components, the standard approach, namely to give an appropriate curvature of the lenses surfaces in order to obtain the required optical properties such as, for instance, a small focal distance is not applicable anymore, new solutions being required.

The first solution is to employ metasurfaces [4, 6] which are arrays of micro/nano antennas each of them having resonant behavior modeling the response of the optical field. The structure of the metasurface is configured in such a way that it controls the shape of the generated light wavefront. In order to generate the desired wavefront, metasurfaces must fulfil the condition requiring that the sizes of the antennas as well as the distance between them must be much smaller than the wavelength at which they operate implying that the sizes of the antennas are in the range of hundreds of nanometers. While this approach is technologically feasible, sometimes it requires a fabrication overhead which might render it more difficult to apply for mass production.

The second solution is to use standard Fresnel lenses [7–11] which are optical components whose optical surfaces are similar to the surfaces of the bulk optical lenses up to a height of the optical path which gives rise to a phase difference of 2π. This is illustrated in Fig.1 where the conversion of a divergent concave bulk lens (Fig. 1 (a)) into its Fresnel counterpart (Fig. 1 (b)) is shown. Fresnel lenses present a series of advantages in terms of reduced weight and thickness, low cost and ease of fabrication in comparison with bulk lenses. At the same time, they have very strong chromatic dispersion preventing their usage in LWIR imaging systems, although higher order diffraction Fresnel lenses where the level heights induce phase difference that are multiple of 2π mitigate somehow the chromatic dispersion effects [8, 9].

Another approach for Fresnel lenses in LWIR imaging instrumentation is to use them as image correctors. Essentially, the imaging system is constructed using standard off the shelf bulk optical components presenting their intrinsic optical dispersion, the role of the correcting Fresnel lens being to compensate and even cancel the aberrations. The Fresnel corrector element presents a large focal length and, implicitly a small optical power, which leads to a small chromatic aberration. Also, it has a small thickness which implies a small attenuation leading to the possibility to use a material such as silicon for its fabrication.

There are two micro-fabrication methods applied to obtain silicon Fresnel lenses. The first one consists in using grey scale lithography to configure the structures [12], followed, in some cases, by etching processes [13]. The second approach, is to use n standard photolithographic

processes in order to configure a Fresnel lens with 2^n depth levels, each process being followed by a reactive ion etching [14].

In this article we present and describe in detail the technological processes necessary to fabricate a silicon image correcting Fresnel lens presenting 16 height levels necessary to approximate the surface of the equivalent bulk element with a good fidelity. We show the discretization process of a divergent concave Fresnel lens and we show the photolithographic masks used in a succession of four standard photolithographic processes. We describe the established and optimized process parameters of deep reactive ion etching necessary [15] to configure the surface of the element. For separating the circular shaped Fresnel lenses from the double polished silicon wafers we employed a Bosch deep etching process [16]. Finally, the backsides of the lenses were thinned by chemical wet etching [17] and both sides of the thin Fresnel lenses were nanopatterned by a metal assisted chemical etching [18] in order to reduce the reflections [19]. The morphological analysis was performed using white light interferometry (WLI) determinations as well as optical and scanning electron microscopy (SEM) imaging revealing that the determined geometrical parameters of the fabricated lenses are in good agreement with designed ones. The infrared spectrometry determinations show that the transmission of the lenses is of 70%.

2. Design and fabrication

The first step in designing a Fresnel lens is to calculate the height level d as the optical path which gives rise to a phase difference of 2π. The height level has to fulfill the following condition $d = \lambda/(n-1)$ where λ is the wavelength and n is the refraction index. This parameter is used to partition the bulk lens in a series of Fresnel zones as shown in Fig.1 where a concave divergent bulk lens Fig. 1 (a) is converted into a Fresnel lens Fig. 1 (b) with three Fresnel zones. For silicon, the refractive index at $\lambda = 9.5\ \mu m$ is $n = 3.417918$ [10] leading to a height d of 3.93 μm.

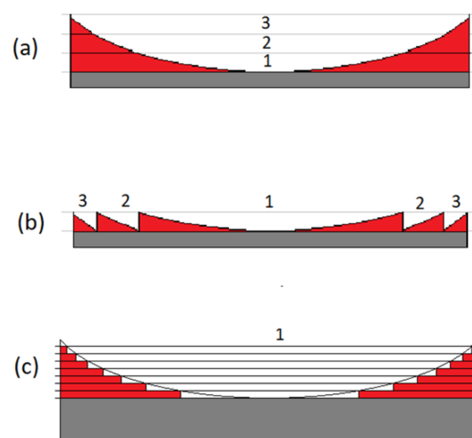

Fig. 1. The procedure to convert a bulk concave lens into a discrete Fresnel lens. (a) the concave surface of the bulk lens. (b) the partition of the bulk lens into three Fresnel zones. (c) discrete first zone of the Fresnel lens. [R. Rebigan et al., "Fabrication of Fresnel lenses operating in long infrared", 2020 International Semiconductor Conference (CAS), Sinaia, Romania, 2020, pp. 133–136, doi: 10.1109/CAS50358.2020.9267996.]

The next step is to convert the smooth continuous surface of the Fresnel lens into a discrete one by partitioning the distance d into 2^n sublevels where n corresponds to the number of the photolithographic masks as it can be seen in Fig. 1 (c) where for clarity purposes only the first zone of the Fresnel lens is shown. In our case the number of photolithographic processes is four such that the number of levels is sixteen. Considering that the Fresnel level d is approximately 4 μm in the spectral range of interest, the height of a sublevel is 250 nm.

The succession of the photolithographic processes is displayed in Fig. 2 where for simplicity we show only three masks. After the first mask is applied on the silicon wafer an etching process configures a $d_1 = d/2$ depth central disk as it shown in Fig. 2 (a). Here the black regions represent the regions covered with photoresist while the white regions represent the windows. For the next photolithographic process the etching depth is $d_2 = d/4$ (Fig. 2(b)), and for the third one the etching depth is $d_3 = d/8$ (Fig. 2 (c)).

Fig. 2. Three photolitographic masks necessary to configure a discrete concave Fresnel lense with eighth levels . (a) first litographic mask, (b) second photolithographic mask, (c) third photolitographic mask [R. Rebigan et al., "Fabrication of Fresnel lenses operating in long infrared", 2020 International Semiconductor Conference (CAS), Sinaia, Romania, 2020, pp. 133–136, doi: 10.1109/CAS50358.2020.9267996.]

The photolithographic masks used for the fabrication of the Fresnel lenses are displayed in Fig. 3, where Fig. 3 (a) - (d) illustrate the photolithographic masks used to configure the Fresnel lenses and Fig. 3 (e) illustrate the photolithographic mask necessary for the separation of the circular shaped Fresnel lenses from the wafer. The masks were realized using CLEWIN software and their geometrical parameters were calculated such that the 16 level discrete lens reproduces with high fidelity the surface of the smooth bulk corrector lens.

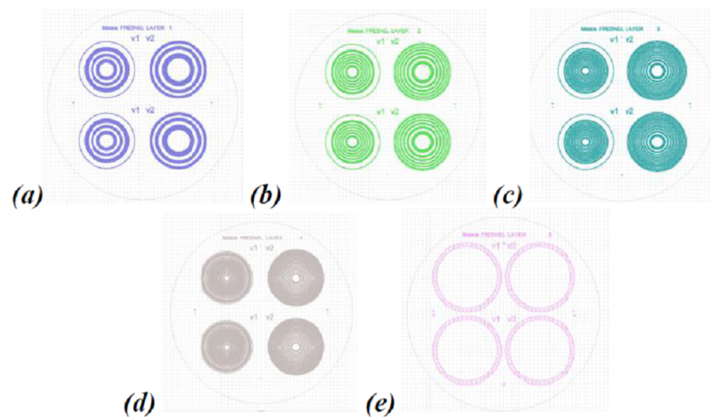

Fig. 3. The photolithographic mask used for the fabrication of the Fresnel lens.(a)-(d) represent the photolithographic masks necessary to configure the surface of the Fresnel lenses (e) the photolithographic masks necessary to separate the Fresnel lenses from the wafer.

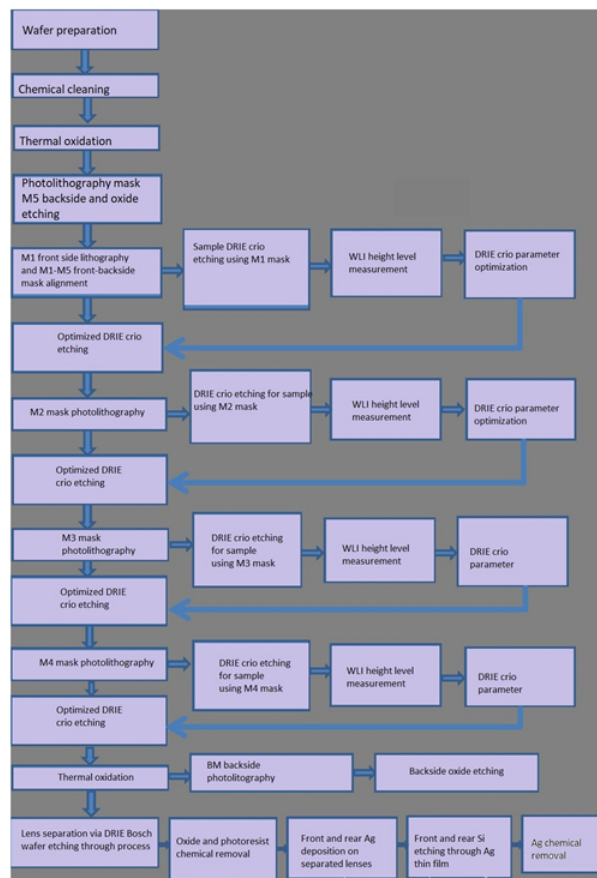

Fig. 4. The complete technological flow necessary for the fabrication of silicon based Fresnel lenses.

Fresnel lenses were fabricated on p (100) double polished Si wafers using photolithographic techniques and deep reactive ion etching DRIE cryogenic plasma etching processes.

The complete technological flow for fabrication of the Fresnel lenses is illustrated in Fig. 4 which is self – explanatory. In the following, the main steps of the fabrication will be explained with the focus upon the configuration of the lenses surfaces.

Essentially, it consists in four photolithographic processes each of them followed by a reactive ion etching. Etching depth corresponding to each photolithographic process are 2 μm, 1 μm, 500 nm and 250 nm. DRIE cryogenic dry plasma etching processes were developed and optimized individually for each etching depth considering the lowest possible controllable etching rate with maximum precision of etching depth in order to conform to design and simulation requirements: minimal roughness of etched silicon areas, vertical walls of etched profile, precise control of each etching depth [14].

The details of the optimized DRIE etching processes with the depths of 2 μm, 1 μm, 0.5 μm and 0.25 μm are listed in Tab. 1. For each photolithographic - etching individual step the processes were developed and optimized considering the LWIR lens requirements such as smooth etched surfaces and vertical steep walls.

Essentially, we employed a DRIE cryogenic etching process at the temperature of – 110°C using SF_6 and O_2 etching gases in a 8% volumetric ratio for the steps of 2 μm and 1 μm and SF6, only, for the steps of 0.5 μm and 0.25 μm, respectively. For the steps of 2 μm and 1 μm, this cryogenic etching process is highly anisotropic due to etching gas O_2 and the low process temperature which leads to the formation of a passivation layer such as SiO_xF_y. This plasma etching process was chosen due to its unique advantages – clean process (no residual chemical products), smooth vertical walls of etched samples, aspect ratio 30:1, etching rate > 5 μm/min using as mask layer thick photoresist or SiO_2 [15, 16].

Table 1. DRIE cryogenic process parameters

DRIE criogenic etching process	**Etched step 2 μm**	**Etched step 1 μm**	**Etched step 500 nm**	**Etched step 250 nm**
ICP Power (W)	1200	1200	450	450
SF_6O_2	8:1	8:1	No O_2	No O_2
P(mtorr)	7,5	7,5	3	3
Etch rate	2,28 μm /min	2,28 μm /min	120 nm/min	120 nm/min
Time	1 min	40 s	4 min	2 min
Temperature (°C)	-115°C(+/- 1°C)	-115°C(+/- 1°C)	-115°C(+/- 1°C)	-115°C(+/- 1°C)

After fabrication, individual Fresnel lenses were separated from the wafer by employing a deep reactive ion etching (DRIE) Bosch process, etching the entire thickness of the wafer. DRIE Bosch etching process parameters are listed in Tab. 2 for each step cycle – the deposition step and the etching step, respectively. The overall etching parameters are: etching rate per cycle 3.4 μm/min, total etching time – 155 min. The photolithographic mask used for the photolithographic process that preeceded the etching process is M_5.

Table 2. DRIE Bosch etching process parameters for individual lens separation from the wafer

Deposition step	**Etching step**
- C_4F_8 flow: 100 sccm;	- C_4F_8 flow: 1 sccm;
- SF_4 flow: 1 sccm;	- SF_6 flow: 100 sccm;
- ICP power: 700 W;	- ICP power: 1100 W;
- RF power 10 W;	- RF power 25 W;
- pressure 20 mT;	- pressure 20 mT;
- time 5 sec./deposition step	- time 12 sec./etching step

The separated Fresnel lenses after complete etching of the wafer depth are shown in Fig. 5.

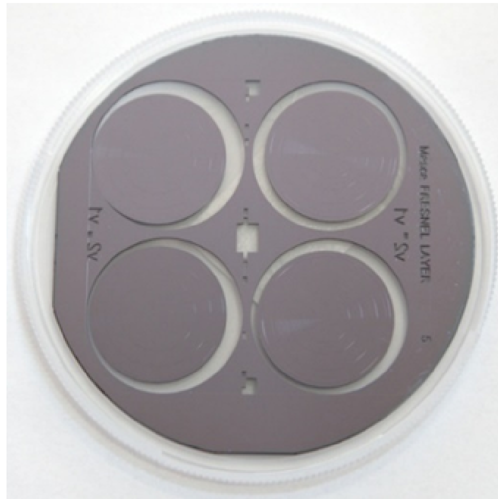

Fig. 5. Image of the Fresnel lenses separated from the wafer by a DRIE Bosch etching

Another important step necessary to fabricate a silicon Fresnel lens with good transmission is the thinning of the silicon wafer. This step, which for reasons of simplicity, is not shown in Fig. 4 is done in order to decrease the attenuation of the lens, which is due to the presence of strong silicon band absorption at the wavelength of 9.5 μm. In our case, the processed samples namely the lenses made out of Silicon p (100) double side polished wafers have a thickness of 530 μm. These samples were thinned using KOH wet etching.

Anisotropic silicon wet etching was performed using KOH for 35-40% concentration in H_2O at 80°C, with approximatively 1 μm/min etching rate. The etched samples feature a small roughness of silicon etched surfaces compared to other concentrations of KOH solutions and different temperatures [17]. Separated individual Fresnel lens were thinned from 530 μm to 270 μm by KOH etching. The front of the Fresnel lenses was protected with a thick SiO_2 and Cr/Au layer and the etching being done on the backside surface of the lenses. Etching KOH solution was chosen considering concentration and temperature aiming at smallest roughness possible for the silicon etched surface and reasonable total etching time for wafer thinning.

Samples were etched using 40% KOH solution at 80°C, with 1.1 μm/min silicon etching rate, and 236 min total etching time. Etching has been performed in a thermostatic bath using magnetic stirrer and thermocouple for temperature control – Fig. 6. After sample thinning, SiO_2 and Cr/Au as protective etching layers have been chemically removed.

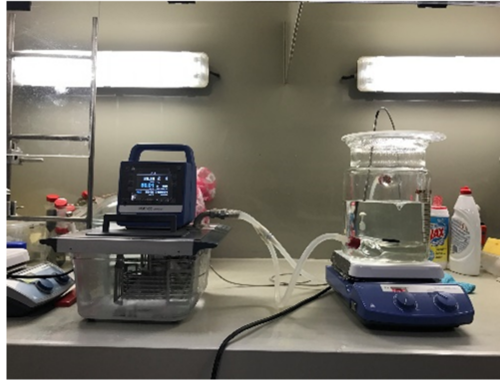

Fig. 6. Thermostatic bath for silicon etching in KOH

To further increase the transmission of the lenses we applied antireflective layers consisting in the porosification of both surfaces of the lens. In this way the surfaces are nanostructured such that their effective refractive index is smaller than the one of the silicon so they act as antireflective layers. The nanostructuring of the surfaces was performed using the metal assisted chemical etching (MACE) [18] method with a chemical solution consisting of HF (5M): H_2O_2 (0.44M) using thin discontinuous metallic layer (Ag/ Au). The details of the design, realization of the antireflective layers , the technological processes as well as the comparison between the transmission spectral characteristics of the samples with and without the antireflective layers are presented elsewhere [19]. Here, we present in Fig. 7 the comparison between the transmission spectral characteristics for a thinned lens with antireflective layers in comparison with a lens which was not thinned with antireflective layers, comparison which shows an increase in the transmission of the thinned lenses in the spectral ranges of 9 μm – 20 μm. Transmittance was measured with a FTIR Vertex 80/80 Brucker Optics Spectrometer operating in the transmission mode. In the spectral range of interest transmittance increased with 10% for the thinned lens with thickness of 270 nm in comparison with the one which did not undergo the thinning process having the thickness of 540 nm.

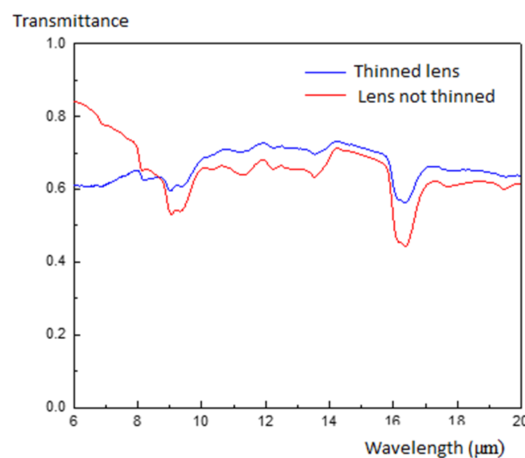

Fig. 7. The transmittance of thinned Fresnel lens presenting antireflective layers on both sides (blue line) in comparison with the transmittance of a (lens which was not thinned red line).

In order to examine the surface of the Fresnel lenses we performed both optical and scanning electron microscopy. Fig. 8 shows the optical microscopy image of the Fresnel lens featuring concentric levels presenting a clear delimitation between them.

Fig. 8. Optical microscopy image of the Fresnel lens

In order to ascertain the agreement between the designed form of Fresnel lenses and the actual one, we performed a complete WLI analysis featuring measured heights of each Fresnel level. Fig. 9 (a) shows the 3-dimensional map of the lens as well as the cross-section measurements Fig. 9 (b) of the first Fresnel zone. At the first glance, the 3D map of the surface shows that the fabricated lens presents a concave form in agreement with the design. A more quantitative analysis can be done by inspecting the cross -section determinations. It can be seen that the height of each of the discreet levels is approximately 250 nm as it is required by the design parameters.

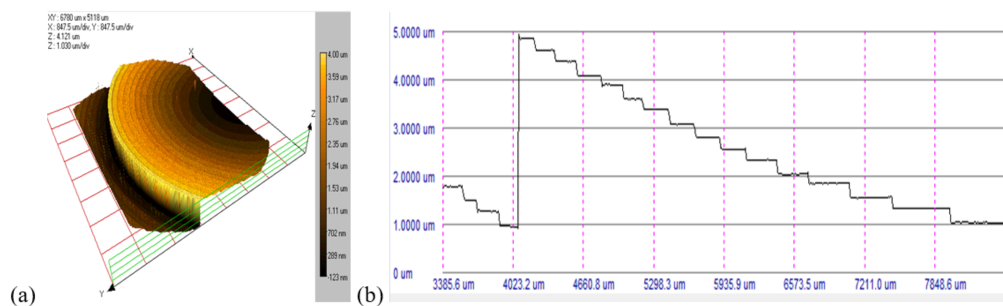

Fig. 9. WLI analysis of the Fresnel lens surface: (a) 3-Dimensional map, (b) cross section with height measurements

3. Conclusions

In conclusion, we developed optimized and tested a complete technological process for fabrication of silicon Fresnel lenses operating as image correctors in LWIR spectral range. The core of the fabrication process consists in the configuration of the optical surfaces of the concave Fresnel lenses, configuration which is done by performing four photolithography steps each of them followed by a DRIE process such that one obtains discreet sixteen level optical components. Additionally, other technological operations consist in the separation of the configured Fresnel lenses from the wafer by a DRIE Bosch process, the thinning of the lenses by a chemical wet process, and the nano-configuration of the both surface of the lenses in order to obtain antireflective layers by a MACE process. The morphological characterizations reveal that the depth profiles of the fabricated lenses are in good agreement with the designs. The functional characterization was performed by determined the transmission spectral characteristics in LWIR which shows that the fabricated lenses present a transmittance above 70%.

Acknowledgements. This work was supported by POC Project TGE – PLAT, Contract no. 77/08.09.2016, subsidiary contract C772D, "High quality image forming optical system with optical diffractive elements in LWIR spectral range, for multi – sensing systems – SOFID"

References

[1] M. VOLLMER, K.-P. MOLLMANN, *Infrared Thermal Imaging: Fundamentals, Research and Applications*, (Wiley, 2017) .

[2] R. SOREF, *Mid-infrared photonics in silicon and germanium*, Nat. Photon. **4**, 495–497 (2010).

[3] G. J. LEE, H. M. KIM, Y. M. Song, *Design and Fabrication of Microscale*, Thin-Film Silicon Solid Immersion Lenses for Mid-Infrared Application, Micromachines **11**, 250 (2020).

[4] S. BANERJI *et al.*, *Imaging with flat optics: Metalenses or diffractive lenses?*, Optica **6**, 805–810 (2019).

[5] Ang WANG, Zhemin CHEN and Yaping DAN, *Planar metalenses in the mid-infrared*, AIP Advances **9**, 085327 (2019).

[6] Qingbin Fan, Mingze Liu, Cheng Yang, Le Yu, Feng Yan, and Ting Xu, *A high numerical aperture, polarization-insensitive metalens for long-wavelength infrared imaging*, Appl. Phys. Lett. **113**, 201104 (2018).

[7] Max BORN and Emil WOLF, *Principles of Optics. Electromagnetic Theory of Propagation, Interference and Diffraction of Light*, 6th Edition, Cambridge University Press 1980.

[8] Monjurul MEEM *et al.*, *Broadband lightweight flat lenses for long-wave infrared imaging* PNAS **116** 21375–21378 (2019).

[9] Tatiana Grulois, *et al.*, *Extra-thin infrared camera for low-cost surveillance applications*, Opt. Lett. **39**, 3169-3172 (2014).

[10] Tatiana Grulois, et al., *Conception of a cheap infrared camera using a Fresnel lens*, Proc. of SPIE **9192** 91920D-2.

[11] Ahmad Rosli Abdul MANAF, Tsunetoshi SUGIYAMA, and Jiwang YAN, *Design and fabrication of Si-HDPE hybrid Fresnel lenses for infrared imaging systems*, Opt. Express **25**, 1202–1220 (2017).

[12] Cheng-Po CHEN, Jason KARP, Tim TOEPFER, Oliver BOOMHOWER, Jim KRETCHMER, Shubhodeep GOSWAMI, Sachin DEKATE, Loucas TSAKALAKOS, *Silicon Fresnel lens fabricated using greyscale lithography*, Proc. SPIE 11104, Current Developments in Lens Design and Optical Engineering XX, 111040G (30 August 2019);

[13] MORGAN B., WAITS C.M., GHODSSI R., *Development of a Deep Silicon Phase Fresnel Lens Using Gray-Scale Lithography and Deep Reactive Ion Etching* Microelectromechanical Systems, Journal of. **13**. 113pp120, (2004). 10.1109/JMEMS.2003.823220.

[14] R. REBIGAN et al., *Fabrication of Fresnel lenses operating in long infrared*, 2020 International Semiconductor Conference (CAS), Sinaia, Romania, 2020, pp. 133–136, doi: 10.1109/CAS50358.2020.9267996.

[15] https://www.oxford-instruments.com/products/etching-deposition-and-growth/processes/etching-processes/silicon/si-cryo-etch

[16] R Dussart1, T Tillocher, P Lefaucheux, M Boufnichel, *Plasma cryogenic etching of silicon: From the early days to today's advanced technologies*, J. Phys. D: Appl. Phys. **47**, 123001, (2014).

[17] John J. KELLY, Harold G.G. PHILIPSEN, *Anisotropy in the wet-etching of semiconductors*, Current Opinion in Solid State and Materials Science **9**, 84pp90, (2005).

[18] Hee HAN, Zhipeng HUANG, Woo LEE, Metal-assisted chemical etching of silicon and nanotechnology applications Nano Today **9**, 271 (2014).

[19] R. REBIGAN, et al Nanostructured silicon based antireflective layers for thermal infrared optical components J. of Optoelectronics and Advanced Materials 22, 136 - 142 (2020).

[20] D. SALZBERG and J. J. VILLA, *Infrared Refractive Indexes of Silicon*, Germanium and Modified Selenium Glass, J. Opt. Soc. Am. **47**, 244–246 (1957).